Distortion of Host Lattice in Clathrate Hydrate as a Function of Guest Molecule and Temperature

Tomoko Ikeda* and Shinji Mae

Department of Applied Physics, Faculty of Engineering, Hokkaido University, Sapporo 060-8628, Japan

Osamu Yamamuro and Takasuke Matsuo

Department of Chemistry, Graduate School of Science, Osaka University, Osaka 560-0043, Japan

Susumu Ikeda

Institute of Materials Structure Science, High Energy Accelerator Research Organization (KEK), Tsukuba, Ibaraki 305-0801, Japan

Richard M. Ibberson

ISIS Science Division, Rutherford Appleton Laboratory, Chilton, Didcot, Oxfordshire, OX11 0QX, U.K.

Received: April 4, 2000; In Final Form: August 8, 2000

Neutron powder diffraction data of deuterated clathrate hydrates of carbon dioxide and xenon were measured in order to investigate the effects of the motion of guest molecules on the structure of the surrounding hydrogen-bonded network. Rietveld analysis revealed that the magnitude of the thermal parameters of the host atoms of the CO_2 clathrate hydrate depends strongly on the crystallographic site, while those of the Xe clathrate hydrate do not depend on the site. The host lattice structure of the Xe clathrate hydrate may be a close representation of the hypothetical empty clathrate hydrate, because of the simple spherical shape of the Xe molecule. The site dependence of the thermal parameters of the host atoms in the CO_2 clathrate hydrate are attributed to the motion of the CO_2 molecules in the cages. The CO_2 molecule rotates anisotropically about the symmetry axis inside the tetrakaidecahedral cage. We suppose that the surrounding deuterium atoms are temporarily attracted and released by the oxygen atoms of the rotating CO_2 molecule and so their thermal parameters are large. It is concluded that the interaction between the guest molecule and the surrounding host atoms is so strong that the thermal vibrations of the host atoms are affected by the motion of the guest molecules inside the cages.

Introduction

Clathrate hydrates[1] are inclusion compounds consisting of water molecules and a variety of guest molecules. The water molecules in clathrate hydrate are linked together by hydrogen bonds in the closest packing of polyhedral cage-like structures (host lattice), which can accommodate guest molecules. The host lattice of the clathrate hydrate consists of the tetrahedral structure and has a proton-disordered arrangement as in various ice polymorphs. The arrangement of protons is described by the equal distribution of protons among the two possible sites on each O−O bond according to the ice rules:[2] (1) there is only one proton on each bond, and (2) there are only two protons close to each oxygen nucleus. Most clathrate hydrates form one of two distinct crystallographic structures, Stackelberg's type-I and −II,[3] depending on the sizes and shapes of the guest molecules. The host lattices, which are less stable than ice, are stabilized by the van der Waals interaction between the guest and host molecules.

McMullen and Jeffrey[4] determined the crystallographic structure of the host lattice in the type-I clathrate hydrate from X-ray diffraction study of ethylene oxide (EtO) clathrate hydrate at 243 K. The cubic unit cell of dimensions $a = 12.03$ Å in space group $Pm3n$ contains 46 water molecules in a framework of two dodecahedral and six tetrakaidecahedral cages. If the cages are fully occupied, the composition is $G{\cdot}5.75H_2O$. Figure 1a,b shows the arrangements of the oxygen and deuterium atoms of the dodecahedral and tetrakaidecahedral cages in the type-I deuterated clathrate hydrate. There are three crystallographically nonequivalent oxygen atoms in sets of 6, 16, and 24 designated as types O_c, O_i, and O_k; k is further classified to k_1 and k_2 by distance from the center of the tetrakaidecahedral cage.[4] The deuterium atoms are equally distributed among the two possible sites on each O−O bond according to the ice rules. There are six crystallographically nonequivalent deuterium atoms: D_{ii}, D_{ck}, D_{kc}, D_{kk}, D_{ki}, and D_{ik}.[5]

The crystallographic structure of the host lattice in the type-II clathrate hydrate was determined by Mak and McMullan[6] from X-ray diffraction data on the double clathrate hydrate of tetrahydrofuran and hydrogen sulfide at 253 K. The cubic unit cell of dimensions $a = 17.31$ Å in space group $Fd3m$ contains 136 water molecules in a framework of 16 dodecahedral and eight hexakaidecahedral cages. If the cages are fully occupied, the composition is $G{\cdot}5.67H_2O$. There are three crystallographi-

* Corresponding author. Present address: Institute of Low-Temperature Science, Hokkaido University, Sapporo 060-0819, Japan. Fax: +81-11-706-7142. E-mail: tomo@hhp2.lowtem.hokudai.ac.jp.

10.1021/jp001313j CCC: $19.00
Published on Web 10/21/2000

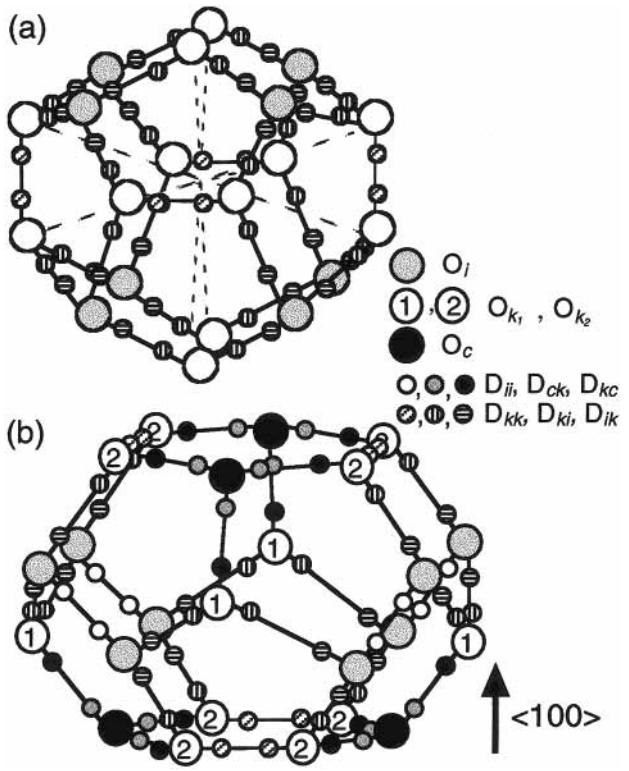

Figure 1. Polyhedral frameworks in the type-I clathrate hydrate: (a) dodecahedral cage and (b) tetrakaidecahedral cage.

cally nonequivalent oxygen atoms in sets of 8, 32, and 96 designated as types O_a, O_e, and O_g. The deuterium atoms are equally distributed among the two possible sites on each O−O bond according to the ice rules. There are six crystallographically nonequivalent deuterium atoms: D_i, D_{1g}, D_{2g}, D_{3g}, D_{1e}, and D_{2e}.[7]

The clathrate hydrates are a kind of nonstoichiometric compounds, whose composition changes depending on temperature and pressure. The phase equilibrium and the thermodynamic stability of the clathrate hydrate has been predicted by the theory of van der Waals and Platteeuw.[8] This theory is based on a model in which the guest molecules are dissolved or adsorbed in the host water lattice as ideal solutions. However, there is a slight but not a negligible discrepancy between the theoretically predicted and experimentally obtained dissociation pressures for most of the guest species.[1] Molecular dynamics simulations showed that the guest−water interaction is the primary factor for stability of the host lattice which is unstable if it is empty.[9−12]

To investigate the mechanism of the guest−water interaction in the clathrate hydrate, several studies have been done. Bertie and Jacobs[13,14] measured X-ray powder diffraction patterns and far-infrared spectra of the type-I clathrate hydrates of Xe, EtO, trimethylene oxide, and cyclopropane, and found that the cubic lattice constant and the vibration energy of the translational lattice vibration mode of the clathrate hydrate depend on the size of the guest molecule. These results showed that the host lattice is distorted by the accommodation of the guest molecules. Using infrared spectroscopy, Fleyfel and Devlin[15] found that the O−D antisymmetric stretching mode of the trimethylene oxide clathrate hydrate splits into two distinct peaks, and attributed the splitting to two subsets of the hydrogen bonds. This result suggests that a strong guest−water interaction in the trimethylene oxide clathrate hydrate causes the disproportionate length of the hydrogen bond in the host lattice. Tse et al.[16] measured incoherent inelastic neutron scattering spectra of the type-I Xe clathrate hydrate and the type-II krypton clathrate hydrate, and found that the transverse acoustic modes of the translational lattice vibrations of these clathrate hydrates are prominent and shifted to high frequencies in comparison with that of the ice Ih. They concluded that the results are attributed to a repulsive guest−host interaction. It was suggested that strong coupling between the localized low-frequency vibrations of the guest molecules and the acoustic phonons of the host lattice greatly enhance the phonon-scattering process. The low-frequency vibrations of the guest molecules can be decomposed into two contributions: the localized translational motion of the center of mass, and the rotation oscillation about this center.[17] The latter occurs for diatomic and polyatomic guest molecules.

The type-I CO_2 clathrate hydrate is suitable for investigation of the guest−host interaction, since the CO_2 molecule is simple in shape. Using NMR spectra, Ratcliffe and Ripmeester[18] showed that the CO_2 molecules in the CO_2 clathrate hydrate occupy only the tetrakaidecahedral cage and rotate about the symmetry axis of the cage. However, Fleyfel and Devlin[15,19] reached a different conclusion by infrared spectroscopy that the CO_2 molecules occupied both the dodecahedral and the tetrakaidecahedral cages, and Ripmeester and Ratcliffe[20] recognized that the NMR data indicates the population of the small cage by CO_2 molecule. To investigate the effect of the cage structure on the motion of the guest molecules, Ikeda et al.[21] measured the crystal orientation dependence of Raman spectra of a single crystal of the type-I CO_2 clathrate hydrate. They found that the scattering intensities of the peaks, which are caused by Fermi resonance of the symmetric stretching mode and the overtone of the bending mode of the CO_2 molecules and the O−H symmetric stretching vibrational mode, vary with variation of the input polarization. Since the results were consistent with the results obtained from measurements of Raman spectra of a single crystal of the type-II natural air clathrate hydrate in a polar ice sheet,[22] they concluded that the uniaxial molecules in the cages rotate anisotropically and that the surrounding water molecules are affected by the motion of the uniaxial guest molecules.

Neutron powder diffraction provides information on the motion of the guest molecules through the spatial distribution of the molecules. It also gives the thermal parameters of the same kind of atoms at crystallographically distinct sites in the host lattice. Yamamuro et al.[23] performed neutron powder diffraction study on deuterated clathrate hydrates of tetrahydrofuran and acetone, and found the preferred orientations for the tetrahydrofuran and acetone molecules in the cages by Rietveld analysis. Kuhs et al.[24] performed neutron powder diffraction on deuterated clathrate hydrate of N_2 using a high-gas-pressure cell and found the pressure dependence of the occupancies of the guest molecules for both of the cages.

Ikeda et al.[25] measured neutron powder diffraction data of deuterated CO_2 clathrate hydrate. They found that the CO_2 molecule in the tetrakaidecahedral cage rotates rapidly even at low temperature, while the rotational motion of the CO_2 molecule in the dodecahedral cage is suppressed with decreasing temperature. They also obtained preliminary data on the site dependence of the thermal parameters of deuterium atoms in the host lattice. They concluded that these results might indicate the strong guest−host coupling in CO_2 clathrate hydrate. Even though the conclusion reached by Ikeda et al.[25] is genuine, limitation of their data set as to the resolution and the sample temperature did not allow a deeper analysis.

The purpose of the present study is to investigate the thermal parameters of the guest and host atoms using more high-

resolution powder diffractometer than before. We have measured deuterated clathrate hydrates of CO_2 and Xe, both which have the type-I structure. The Xe clathrate hydrate was studied along with the CO_2 clathrate hydrate, because comparison of these two would enhance any effects associated with the rotation of the CO_2 molecules in the lattice.

Experimental Section

A powder sample of deuterated Xe clathrate hydrate was prepared in the following manner. To provide a large reaction surface, 13 g of D_2O ice Ih was finely ground. The powder ice was loaded into a pressure cell and pressurized with Xe gas to 1.8 MPa at 250 K. To accelerate the hydrate formation, the sample temperature was cycled between 250 and 278 K. The formation rate became slow after several days, probably because unreacted ice was covered by the formed hydrate. To provide a new reaction surface, the sample was ground in a glovebox under Xe gas at 200 K. The ground sample was loaded into the pressure cell and pressurized with Xe gas again. The above procedure was repeated several times in about two months. Then, the sample was kept at 251 K under a Xe gas atmosphere of 1.9 MPa for about two months to homogenize the guest occupancy. From the ideal solution model and the Langmuir constants,[26] the Xe occupancy (at 251 K, 1.9 MPa) was estimated to be 1.00 for both of the cages. The composition of the sample for full occupancy was $Xe{\cdot}5.75D_2O$.

For a sample of deuterated CO_2 clathrate hydrate, the powdered D_2O ice was pressurized with CO_2 gas to 2.0 MPa at 253 K. The sample temperature was cycled between 253 and 277 K. After several days, the sample was ground in a glovebox under CO_2 gas at 200 K and pressurized with CO_2 gas again. The above procedure was repeated several times in about two months. Then, the sample was kept at 198 K under a CO_2 gas atmosphere of 0.1 MPa for about two months. From the ideal solution model and the Langmuir constants,[27] the CO_2 occupancies (at 198 K, 0.1 MPa) were estimated to be 0.99 and 1.00 for the dodecahedral and tetrakaidecahedral cages, respectively. The composition of the sample was calculated to be $CO_2{\cdot}5.76D_2O$.

Full data of neutron diffraction for refinements were measured at 5, 70, 140, and 205 K for CO_2 clathrate hydrate and at 5, 70, 140, 205, and 259 K for Xe clathrate hydrate. The lattice constants of CO_2 clathrate hydrate were measured in the temperature range 5−195 K at intervals of 10 K. The data were collected on the high-resolution powder diffractometer (HRPD) installed at the ISIS pulsed neutron source at the Rutherford Appleton Laboratory. The resolution ($\Delta d/d$) of this apparatus is 0.05%,[28] which is much better than that of Vega (0.2%) used in the preliminary measurements.[25] Structure parameters were refined by the Rietveld method[29] using intensity data between $d = 0.7$ and 2.3 Å. The used computer program was REFINE developed by the powder diffraction group.[30]

Results and Discussion

Xe Clathrate Hydrate. Figure 2 shows the neutron diffraction pattern of the Xe clathrate hydrate at 5 K. The plus marks denote the observed intensities; the solid line was calculated for the best-fit model described below. The peak positions calculated from the refined structure are shown by tick marks below the diffraction pattern.

The structure of the EtO clathrate hydrate determined by neutron diffraction[5] was used for the initial model of the host lattice. The atomic coordinates for the Xe molecules were fixed to the values at the centers of the cages. The final values of χ^2 were 1.74, 1.68, 1.49, 1.35, and 1.38 at 5, 70, 140, 205, and 259 K, respectively. The fittings were quite satisfactory as shown by the deviation plot in Figure 2. The structure parameters of the final model at 5 K are listed in Table 1. The bond lengths and bond angles of the D_2O molecules were reasonably comparable with the previous studies for the EtO clathrate hydrate.[4,5]

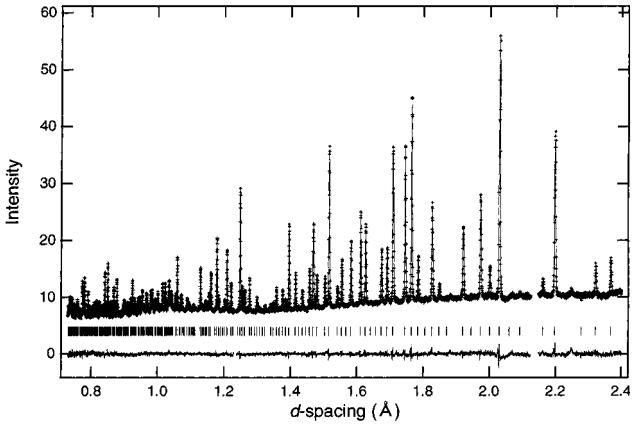

Figure 2. Neutron powder diffraction pattern of the Xe clathrate hydrate at 5 K. The plus marks denote the observed intensities; the solid line is that calculated from the best-fit model of the Rietveld refinement. The tick marks represent the calculated peak positions for the type-I clathrate hydrate (*Pm*3*n*), and the curve below them represents the deviation between the observed and calculated intensities.

TABLE 1: Final Structural Parameters for Xe Clathrate Hydrate at 5 K

atom	x	y	z	occupancy	B (Å^2)
		Host Atoms			
O_i	0.18342(5)	0.18342(5)	0.18342(5)	1	0.462(17)
O_k	0.0000	0.30871(9)	0.11682(9)	1	0.533(18)
O_c	0.0000	0.5000	0.2500	1	0.485(33)
D_{ii}	0.23157(9)	0.23157(9)	0.23157(9)	0.5	1.180(44)
D_{ck}	0.0000	0.43272(19)	0.20190(17)	0.5	1.147(40)
D_{kc}	0.0000	0.37860(20)	0.16036(18)	0.5	1.224(41)
D_{kk}	0.0000	0.31685(15)	0.03436(14)	0.5	1.352(38)
D_{ki}	0.06728(15)	0.26540(12)	0.13872(11)	0.5	1.228(27)
D_{ik}	0.11693(12)	0.22843(12)	0.15861(12)	0.5	1.168(27)
		Guest Atoms			
Xe(1)	0.0000	0.2500	0.5000	1	0.850(40)
Xe(2)	0.0000	0.0000	0.0000	1	0.883(72)

The solid squares in Figure 3 show the temperature dependence of the lattice constant a of the Xe clathrate hydrate. The data are fitted to a quadratic polynomial of the form

$$a(T)\ (\text{Å}) = 11.833 + 4.9692 \times 10^{-5}\, T + 1.7966 \times 10^{-6}\, T^2 \quad (1)$$

as shown by the broken line in Figure 3. T (K) is the temperature. The a of the type-I EtO clathrate hydrate observed by X-ray powder diffraction (open triangles) were also fitted to a quadratic polynomial ($a = 11.835 + 2.2173 \times 10^{-5}\, T + 2.2415 \times 10^{-6}\, T^2$) as shown by the dotted line in Figure 3.[31]

From Figure 3, it can be seen that the thermal expansion of the Xe clathrate hydrate is smaller than that of the EtO clathrate hydrate. Theoretical molecular dynamics calculations showed that the simulated thermal expansion of the hypothetical empty clathrate hydrate (type-I) is small in comparison with the simulated thermal expansion of the EtO clathrate hydrate.[31] Therefore, the present results show that the host lattice structure of the Xe clathrate hydrate is a close representation of the hypothetical empty clathrate hydrate in comparison with that

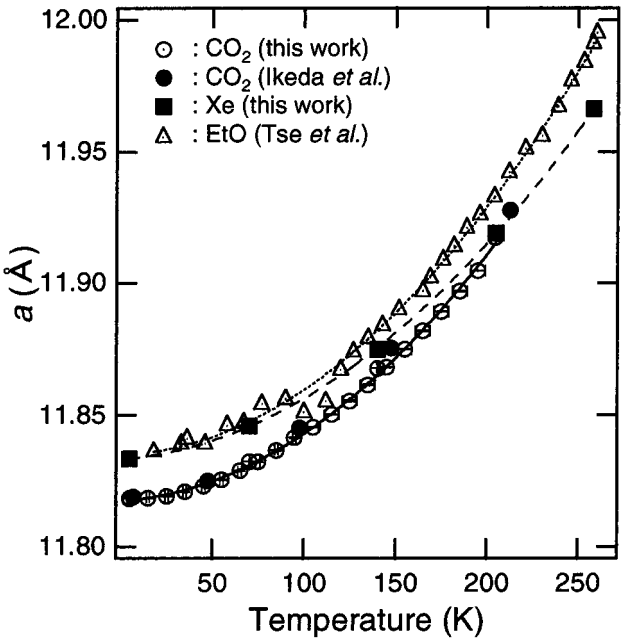

Figure 3. Temperature dependence of the lattice constant *a* of the CO_2 clathrate hydrate (open circles) and the Xe clathrate hydrate (solid squares). The solid circles and open triangles show the reported *a* values of the CO_2 clathrate hydrate[25] and the EtO clathrate hydrate,[31] respectively.

of the EtO clathrate hydrate. The larger thermal expansion in the EtO clathrate hydrate is attributed to interactions between the host lattice and the guest molecules. Because the frequencies of the localized rotational and translational vibrations of the EtO molecules in the cages are very close to those of the lattice acoustic modes,[17] coupling between these vibrations causes the increase in the thermal expansitivity in the EtO clathrate hydrate.

As shown in Figure 3, the thermal expansion of the EtO clathrate hydrate approaches the value of the Xe clathrate hydrate with decreasing temperature. This is attributed to a glass transition in the EtO clathrate hydrate, because the glass transition of the EtO clathrate hydrate was observed at around 90 K in the heat capacity study.[32] Since the rotational motion of the EtO molecules are frozen in the surrounding of the frozen water molecules, the thermal expansion approaches the value of the Xe clathrate hydrate.

The thermal parameter is useful for clarifying the difference of the thermal vibration of the same kind of atoms at crystallographic distinct sites. Figure 4a shows the isotropic thermal parameters, *B*, of the Xe atoms in the tetrakaidecahedral cage (circles) and in the dodecahedral cage (triangles). The *B* parameters of the Xe atoms in both of the cages decrease and approach zero with decreasing temperature, which indicates a negligible small zero-point amplitude. The value of *B* for the Xe atom in the tetrakaidecahedral cage is about two times larger than that in the dodecahedral cage at 259 K. The thermal parameter of an atom is related to its root-mean-square displacement (u) by $B = 8\pi^2u^2$. The *B* value for the Xe atom in the tetrakaidecahedral cage is 8.96(17) Å^2. This can be converted into vibrational amplitude of 0.34 Å. This large amplitude of the thermal vibration of Xe in the tetrakaidecahedral cage in comparison with that in the dodecahedral cage is thought to be due to one of the following: (1) the stable position of the Xe atom deviates from the center of the cage, or (2) the localized translational motion of the Xe atom at the center of the cage. Mechanism (1) can be ruled out, because the *B* parameter of the Xe atom in the tetrakaidecahedral cage approaches 0 with

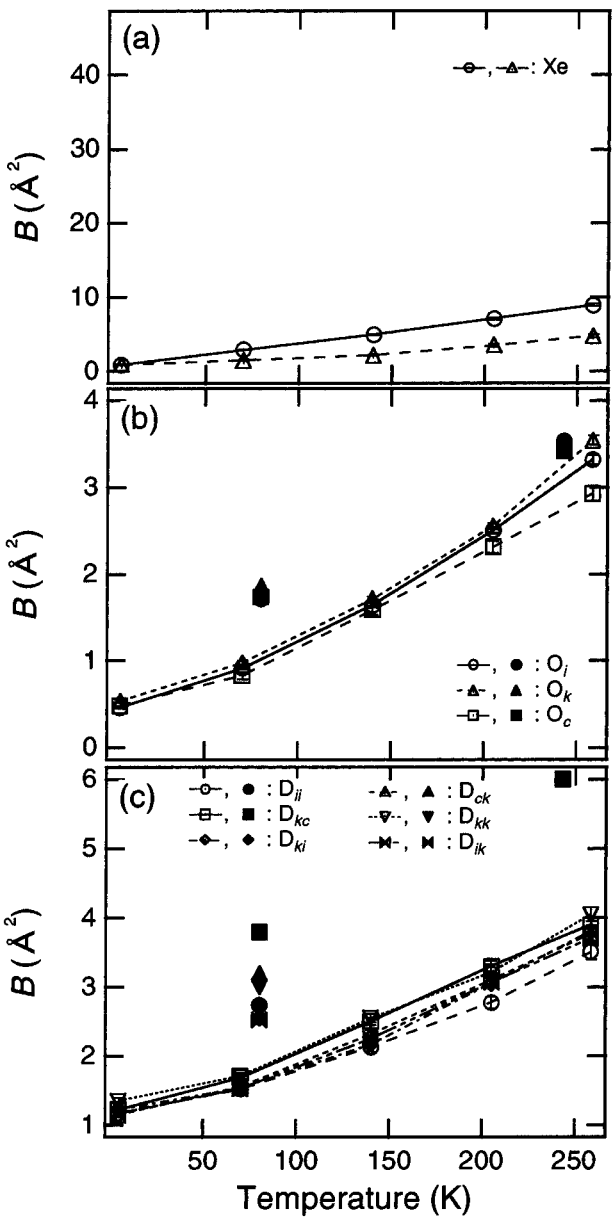

Figure 4. The *B* parameters of the atoms in the Xe clathrate hydrate (open symbols): (a) the Xe atoms in the tetrakaidecahedral and in the dodecahedral cages (circles and triangles, respectively); (b) the oxygen atoms in the host lattice; (c) the deuterium atoms in the host lattice. The solid symbols show the *B* parameters of the EtO clathrate hydrate.[4,5]

decreasing temperature. Because the atomic coordinates for the Xe atoms were fixed to the values at the centers of the cages in our model for the structural refinement, the Xe atom located around the center of the cage should have a high *B* value even at low temperature. Thus, we conclude that the large amplitude of the thermal vibration of the Xe atom in the tetrakaidecahedral cage at the high temperature is attributable to the translational motion of the Xe molecule about the center of the cage.

Figure 4b shows the *B* parameters of the oxygen atoms in the host lattice of the Xe clathrate hydrate. The magnitude and the temperature dependence of the *B* parameter of the oxygen atom do not depend on the site. The *B* values for all the sites decrease with decreasing temperature. Since the EtO clathrate hydrate has the type-I structure, we attempt to compare the present results with the *B* parameters of the EtO clathrate hydrate. The solid symbols in Figure 4b show the *B* parameters of the oxygen atoms in the EtO clathrate hydrate at 80 and 243 K.[4,5] The magnitudes of the *B* parameters of the oxygen atoms

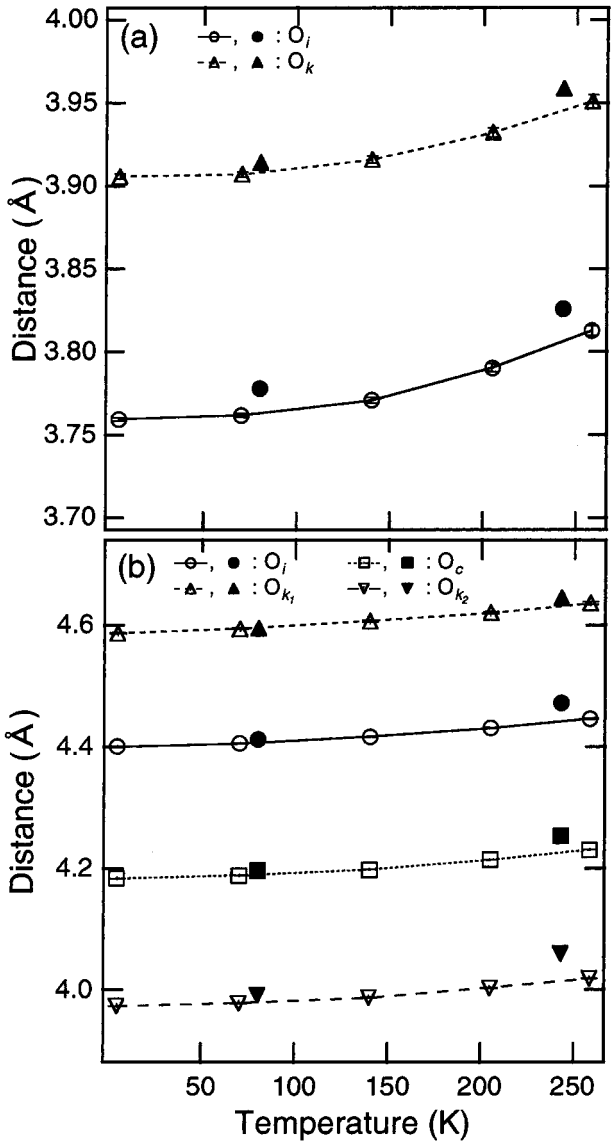

Figure 5. Distances of the oxygen atoms from the centers of (a) the dodecahedral cage, and (b) the tetrakaidecahedral cage in the Xe clathrate hydrate (open symbols). The solid symbols show the distances for the EtO clathrate hydrate.[4,5]

for the EtO clathrate hydrate are larger than those for the Xe clathrate hydrate at 80 K, while the values are almost equal at 243 K. As shown in Figure 5a,b, the average distance between the centers of the cages and oxygen atoms in the host lattice in the EtO clathrate hydrate are almost equal to those in the Xe clathrate hydrate at 80 K. Further, the orientation of the EtO molecule are localized at low temperature. Therefore, the large *B* values for the EtO clathrate hydrate at 80 K are attributable to the distributions of the positions of the oxygen atoms caused by orientational disorder of the localized guest molecules in the cages. At high temperature, the distributions of the oxygen atom positions are small, because the motions of the EtO molecules in the cages are less restricted. The distances from the centers of the cages for all the oxygen atoms in the EtO clathrate hydrate are larger than those in the Xe clathrate hydrate at 243 K. This indicates that the distortions of the cages in the EtO clathrate hydrate from the hypothetical empty clathrate hydrate are small.

Figure 4c shows the *B* parameters of the deuterium atoms in the host lattice of the Xe clathrate hydrate. The magnitude and the temperature dependence of the *B* parameter of the deuterium atom do not depend on the site. The *B* values for all the sites decrease with decreasing temperature. The solid symbols in Figure 4c show the *B* parameters of the deuterium atoms in the EtO clathrate hydrate at 80 and 243 K.[4,5] The magnitudes of *B* for the EtO clathrate hydrate are larger than those for the Xe clathrate hydrate over the whole temperature range. A likely explanation for this is that the large *B* values for the EtO clathrate hydrate at low temperature can be attributed to the distributions of the positions of the deuterium atoms caused by orientational disorder of the localized guest molecules inside the cages. In contrast, the large *B* values for the EtO clathrate hydrate at high temperature are caused by the thermal vibration of deuterium atoms at the average positions. We suppose that the deuterium atoms are temporarily attracted and released by the oxygen atom of the rotating EtO molecule (i.e., $(CH_2)_2O$), so the *B* parameters are large.

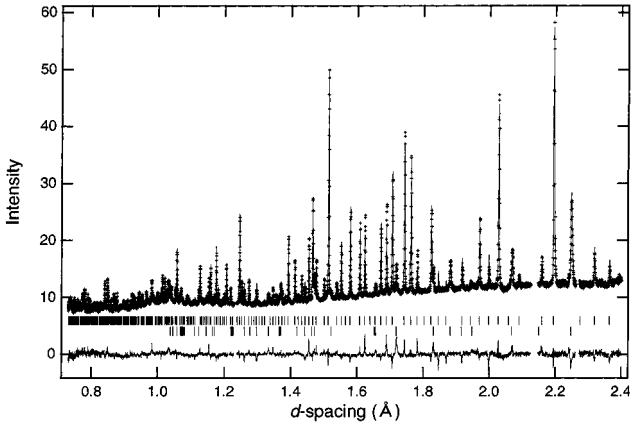

Figure 6. Neutron powder diffraction pattern of the CO_2 clathrate hydrate at 5 K. The plus marks denote the observed intensities; the solid line is that calculated from the best-fit model of the Rietveld refinement. The top and bottom rows of tick marks represent calculated peak positions for the type-I clathrate hydrate (*Pm*3*n*) and for the ice Ih ($P6_3/mmc$), respectively. The curve below them represents the deviation between the observed and calculated intensities.

CO_2 Clathrate Hydrate. The diffraction patterns measured at four temperatures revealed that the sample of CO_2 clathrate hydrate was a mixture of type-I clathrate hydrate (*Pm*3*n*) and a small amount of ice Ih ($P6_3/mmc$). Therefore, multiphase refinement was performed. To reduce the number of adjustable parameters, the atomic coordinates of the ice Ih were fixed to the reported values.[33] The thermal parameters of the oxygen and deuterium atoms in the ice Ih were fixed to the estimates from the reported values at 15, 123, and 223 K.[33,34] Figure 6 shows the neutron diffraction pattern of the CO_2 clathrate hydrate at 5 K. The plus marks denote the observed intensities, and the solid line was calculated for the best-fit model described below. The peak positions for the type-I clathrate hydrate (*Pm*3*n*) and for the ice Ih ($P6_3/mmc$) are shown by tick marks below the diffraction pattern.

The structure of the EtO clathrate hydrate determined by neutron diffraction[5] was used for the initial model of the host lattice. For the CO_2 molecule in the tetrakaidecahedral cage, the initial model was constructed according to the results of the NMR study.[18] The carbon atom was fixed at the center of the cage, and the molecular axis was placed at 31° from the equatorial plane of the cage so as to point to the O_k and O_c atoms of the cage; there are three equivalent orientations. For the orientation of the CO_2 molecule in the dodecahedral cage, the following four models were tested: (A) two oxygen atoms of CO_2 point to O_k of the host lattice as shown by the broken lines in Figure 1a, (B) two oxygen atoms of CO_2 point to the

TABLE 2: Final Structural Parameters for CO_2 Clathrate Hydrate at 5 K

atom	*x*	*y*	*z*	occupancy	*B* (Å^2)
		Host Atoms			
O_i	0.18372(15)	0.18372(15)	0.18372(15)	1	2.566(62)
O_k	0.0000	0.30996(25)	0.11416(25)	1	1.457(47)
O_c	0.0000	0.5000	0.2500	1	0.716(71)
D_{ii}	0.23783(51)	0.23783(51)	0.23783(51)	0.5	3.77(17)
D_{ck}	0.0000	0.43237(54)	0.20468(46)	0.5	2.64(12)
D_{kc}	0.0000	0.38429(58)	0.16541(59)	0.5	3.55(14)
D_{kk}	0.0000	0.31066(32)	0.03230(39)	0.5	2.42(10)
D_{ki}	0.06225(46)	0.26517(36)	0.13684(32)	0.5	3.266(95)
D_{ik}	0.10922(31)	0.23281(28)	0.15462(23)	0.5	1.830(78)
		Guest Atoms			
C(1)	0.0000	0.2500	0.5000	1	39.4(1.6)
O(4)	0.0731	0.3006	0.4584	0.167	28.8(1.5)
O(5)	0.0000	0.3006	0.4159	0.167	28.8(1.5)
C(2)	0.0000	0.0000	0.0000	0.990	2.86(19)
O(6)	0.0000	0.0917	0.0349	0.165	12.8(1.2)

centers of the O_k-O_i bonds, (C) two oxygen atoms of CO_2 point to the centers of the two pentagons, and (D) two oxygen atoms of CO_2 point to the centers of the O_k-O_k bonds. For all the models, the carbon atom was fixed at the center of the cage. The smallest values of χ^2 were obtained for model (A) over the whole temperature range. The atomic coordinates for the CO_2 molecules were fixed to the values described above. The final values of χ^2 were 4.99, 3.79, 3.05, and 2.40 at 5, 70, 140, and 205 K, respectively. The amount of the ice determined by this method was 14.8 $\pm$ 0.2% of the total water content. The structure parameter of the final model at 5 K are listed in Table 2. The bond lengths and bond angles of the D_2O molecules were reasonably comparable with the present study for the Xe clathrate hydrate and the previous studies for the EtO clathrate hydrate.[4,5]

The open circles in Figure 3 show the temperature dependence of the lattice constant *a* of the CO_2 clathrate hydrate. The data are fitted to a quadratic polynomial of the form

$$a = 11.818 + 4.2451 \times 10^{-5}\, T + 2.1238 \times 10^{-6}\, T^2 \qquad (2)$$

as shown by the solid line in Figure 3. Ikeda et al.[25] proposed that the slope (d*a*/d*T*) changes slightly around 100 K by the glass transition due to the freezing of the water reorientational motion. However, we found no change of d*a*/d*T* around 100 K. We conclude that the interpretation of the data in the previous report was caused because they measured *a* at only five selected temperatures. The values of *a* in the previous report are consistent with the present results, as shown by the solid circles in Figure 3.

The *a* of the CO_2 clathrate hydrate is 0.0151 Å smaller than that of the Xe clathrate hydrate at 5 K. The difference in the *a* between the clathrate hydrates of CO_2 and Xe decreases with increasing temperature. From eqs 1 and 2, the *a* of the CO_2 clathrate hydrate is equal to that of the Xe clathrate hydrate at 225 K, and becomes larger than that of the Xe clathrate hydrate above 225 K. The lattice constant of the clathrate hydrate depends on the size of the guest molecule, when the guest molecule rotates isotropically in the cage. The CO_2 molecule rotates isotropically in the large cage at high temperature in comparison with low temperature.[18] The largest van der Waals diameters of CO_2 and Xe molecules are 4.7 and 4.4 Å, respectively. Therefore, when the CO_2 molecules rotate isotropically in the cages, the *a* value of the CO_2 clathrate hydrate is larger than that of the Xe clathrate hydrate. At low temperature, the *a* values do not depend on the largest van der Waals diameters of the guest molecules, because the CO_2 molecules rotate anisotropically in the cages.

From Figure 3, it can be seen that the thermal expansion of the CO_2 clathrate hydrate is much larger than that of the Xe clathrate hydrate at high temperature and approaches the value of the Xe clathrate hydrate with decreasing temperature. This may indicate that the CO_2 clathrate hydrate undergoes the glass transition due to freezing of the reorientational motion of the water molecules at low temperature, even though different vibrational anharmonicity may well explain the observed behavior of the two components. The larger thermal expansion in the CO_2 clathrate hydrate at high temperature is attributed to the strong interactions between the host lattice and the CO_2 molecules.

For the ice Ih, negative thermal expansion has been observed below 73 K.[35] The Grüneisen function in the lattice with a tetrahedral structure is negative at low temperature.[36] However, we found no evidence of negative thermal expansion in the clathrate hydrates of CO_2 and Xe over the temperature region within the limits of accuracy of our measurements. These results are consistent with the results for the EtO clathrate hydrate.[31] Unlike ice Ih, clathrate hydrates may not have a negative Grüneisen function because of distortion of the tetrahedral structures in clathrate hydrates. The deviations of the valence O−O−O angles in clathrate hydrate are considerable in comparison with the ice Ih.

Figure 7 shows the distances of the oxygen atoms from the centers of the cages in the CO_2 clathrate hydrate. From Figures 5a and 7a, it can be seen that the distance of O_k from the center of the dodecahedral cage in the CO_2 clathrate hydrate is larger than that in the Xe clathrate hydrate at high temperature and approaches the value of the Xe clathrate hydrate with decreasing temperature. For O_i, the distances from the center of the dodecahedral cage in the clathrate hydrates of CO_2 and Xe are approximately equal over the whole temperature range. From Figures 5b and 7b, it can be seen that the distance of O_{k_1} from the center of the tetrakaidecahedral cage in the CO_2 clathrate hydrate is larger than that in the Xe clathrate hydrate over the whole temperature range, while that of O_{k_2} is smaller than that in the Xe clathrate hydrate. For O_i and O_c, the distances from the center of the tetrakaidecahedral cage in the clathrate hydrates of CO_2 and Xe are approximately equal. These results indicate that the tetrakaidecahedral cage in the CO_2 clathrate hydrate is distorted along the ⟨100⟩ axis. This distortion is caused by anisotropic rotation of the CO_2 molecule about the ⟨100⟩ axis in the tetrakaidecahedral cage.

Figure 8a shows the *B* parameters of the carbon and oxygen atoms of the CO_2 molecule in the tetrakaidecahedral cage (circles) and in the dodecahedron cage (triangle). The *B* parameters of the atoms in the CO_2 molecule are significantly larger than those of the Xe atoms in the Xe clathrate hydrate (See Figure 4a). The *B* values for the carbon and oxygen atoms of the CO_2 molecule in the dodecahedral cage are 2.86(19) and 12.8(1.2) Å^2, respectively, at 5 K. These can be converted into vibrational amplitudes of 0.19 and 0.40 Å, respectively. The small vibrational amplitude for the carbon atom suggests that the carbon atom, on the average, is located at the center of the dodecahedral cage. The large amplitude of the oxygen atom in the dodecahedral cage may arise from the following: (1) the CO_2 molecule rotates in the cage, and (2) the CO_2 molecule also takes three other orientations (i.e., models (B), (C), and (D)) as metastable states. At high temperature, the large amplitude of the thermal vibration is mainly due to mechanism

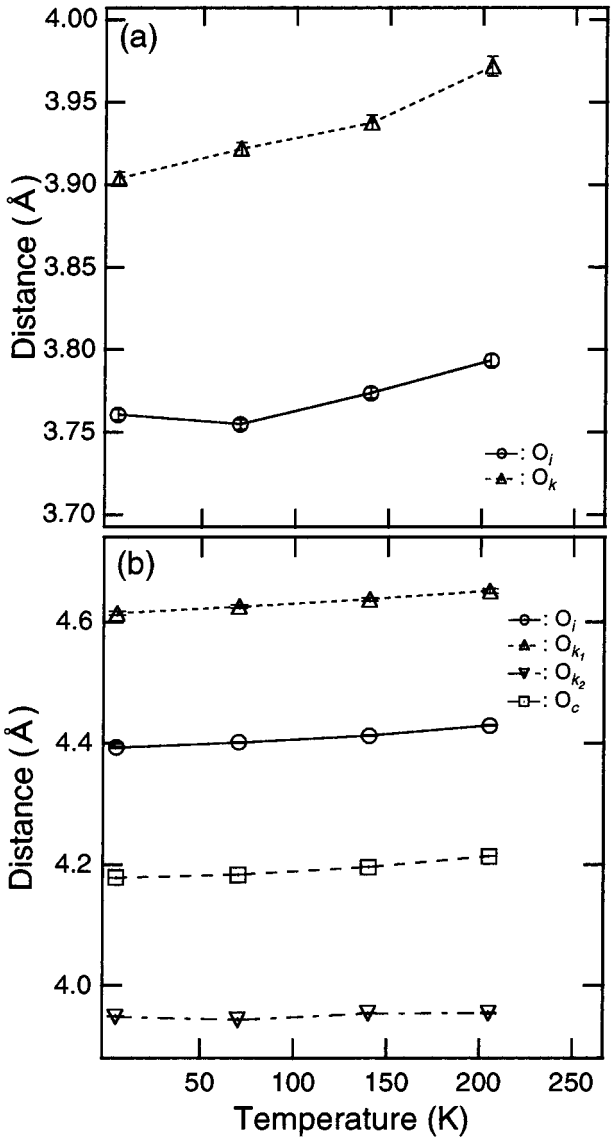

Figure 7. Distances of the oxygen atoms from the centers of (a) the dodecahedral cage, and (b) the tetrakaidecahedral cage in the CO_2 clathrate hydrate.

(1), because the CO_2 molecule does freely rotate in the cage. The rotational motion of the CO_2 molecule is frozen in the surroundings of the frozen water molecules at low temperature. Therefore, the large amplitude of the thermal vibration for the oxygen atom at low temperature is mainly due to mechanism (2).

The *B* parameters for the atoms in the CO_2 molecule in the tetrakaidecahedral cage are large in comparison with those in the dodecahedral cage. The *B* values for the carbon and oxygen atoms of the CO_2 molecule in the tetrakaidecahedral cage are 39.4(1.6) and 28.8(1.5) Å^2, respectively, at 5 K. These are equivalent to vibrational amplitudes of 0.71 and 0.60 Å, respectively. The large vibrational amplitude for the carbon atom suggests that the average position of the carbon atom may not be situated at the center of the cage, because the atomic coordinates for the carbon atoms were fixed to the values at the centers of the cages in our model for the structural refinement. The vibrational amplitude for the oxygen atom is large over the whole temperature range, because the CO_2 molecule in the tetrakaidecahedral cages rotates rapidly, even in the surroundings of the frozen water molecules at low temperature.[18]

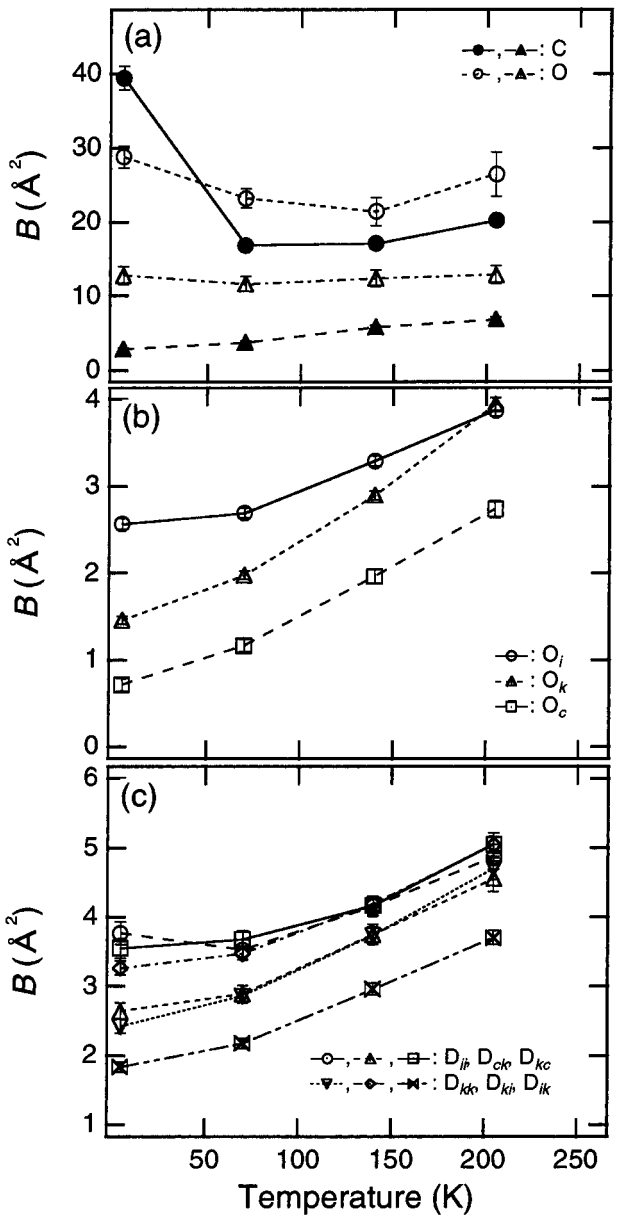

Figure 8. The *B* parameters of the atoms in the CO_2 clathrate hydrate: (a) the carbon and oxygen atoms in the CO_2 molecules in the tetrakaidecahedral and the dodecahedral cages (circles and triangles, respectively); (b) the oxygen atoms in the host lattice; (c) the deuterium atoms in the host lattice.

Figure 8b shows the *B* parameters of the oxygen atoms of the water molecules in the CO_2 clathrate hydrate. The *B* parameters of the oxygen atoms in the CO_2 clathrate hydrate are significantly larger than those in the Xe clathrate hydrate (see Figure 4b), and the magnitude depends strongly on the site. The *B* parameter of O_i is large in comparison with those of O_k and O_c. The large *B* parameter of O_i is associated with the fact that the CO_2 molecule inside the tetrakaidecahedral cage rotates about the symmetry axis (i.e., the ⟨100⟩ axis) of the cage, because the O_i are located around the rotational plane of the CO_2 molecule. The small *B* value of O_k, which are also located around the rotational plane of the CO_2 molecule inside the tetrakaidecahedral cage, may be related to distance from the rotating CO_2 molecule.

Figure 8c shows the *B* parameters of the deuterium atoms in the CO_2 clathrate hydrate. The *B* parameters of the deuterium atoms in the CO_2 clathrate hydrate are significantly larger than those in the Xe clathrate hydrate (see Figure 4c), and the

magnitude depends on the site. The *B* parameters of D_{ii}, D_{kc}, and D_{ki} are larger than those of D_{ck}, D_{kk}, and D_{ik}. The large *B* parameters of the deuterium atoms are also attributed to the rotational motion of the CO_2 molecule inside the cages. D_{ii}, D_{kc}, D_{ki}, and D_{ik} are located around the rotational plane of the CO_2 molecule. D_{ii} and D_{kc} are incorporated only in the tetrakaidecahedral cage, while D_{ki} and D_{ik} are incorporated in both the dodecahedral and the tetrakaidecahedral cages. Thus, the large *B* parameters of D_{ii} and D_{kc} are associated with the fact that the CO_2 molecule inside the tetrakaidecahedral cage rotates about the symmetry axis. We suppose that D_{ii} and D_{kc} are temporarily attracted and released by the oxygen atoms of the rotating CO_2 molecule, so their effective *B* parameters are large. The large *B* value of D_{ki}, which is incorporated in both of the cages, may be related to the rotational motions of the CO_2 molecules inside both of the cages. The CO_2 molecule reorientates (i.e., rotates) so as to point to the two O_k atoms of the host lattice in the dodecahedral cage at high temperature. Since D_{ki} are located around O_k, D_{ki} are temporarily attracted and released by the oxygen atoms of the rotating CO_2 molecules inside both the dodecahedral and tetrakaidecahedral cages, so their effective *B* parameters are large. The rotational motion of the CO_2 molecule in the dodecahedral cage is localized at low temperature. Thus, the large *B* values for the D_{ki} at low temperature can be attributed to the distributions of D_{ki} from the average position due to the orientational disorder of the localized CO_2 molecule inside the dodecahedral cage.

Conclusions

We measured the neutron powder diffraction data of deuterated clathrate hydrates of CO_2 and Xe. Rietveld analysis revealed that the magnitude and temperature dependence of the thermal parameters *B* of the host atoms of the CO_2 clathrate hydrate depend strongly on the crystallographic site, while those of the Xe clathrate hydrate are independent of the site. The site dependencies of the *B* parameters for the CO_2 clathrate hydrate are attributable to anisotropic rotational motion of the CO_2 molecules inside the cages. In contrast, the structure of the host lattice of the Xe clathrate hydrate may more closely represent the hypothetical empty clathrate hydrate, because of the simple spherical shape of the Xe molecule. We conclude that the results show the effects of motion of the guest molecules on the structure of the surrounding hydrogen-bonded network. These effects are attributed to the strong guest−host interactions which are the dominant factor governing the stability of the clathrate hydrate.

Acknowledgment. We thank Dr. T. Kamiyama of the University of Tsukuba, Dr. F. Izumi of National Institute for Research in Inorganic Material, Dr. T. Hondoh, Dr. A. Kouchi, and Dr. H. Fukazawa of Hokkaido University for their valuable discussion. This work was partly supported by a Grant-in-Aid for Scientific Research of the Japanese Ministry of Education, Science and Culture. T.I. and S.M. thank the New Energy and Industrial Technology Development Organization for financial support. One of the authors, T.I., has been supported by a Research Fellowship of the Japan Society for the Promotion of Science.

References and Notes

(1) Sloan, E. D., Jr. *Clathrate Hydrate of Natural Gases, 2nd ed.*; F., Marcel Dekker: New York, 1998.
(2) Pauling, L. *J. Am. Chem. Soc.* **1935**, *57*, 2680.
(3) Stackelberg, M. von; Muller, H. R. *Z. Elektrochem* **1954**, *58*, 25.
(4) McMullen, R. K.; Jeffrey, G. A. *J. Chem. Phys.* **1965**, *42*, 2725.
(5) Hollander, F.; Jeffrey, G. A. J. *Chem. Phys.* **1977**, *66*, 4699.
(6) Mak, T. C.; McMullen, R. K. *J. Chem. Phys.* **1965**, *42*, 2732.
(7) McMullen, R. K.; Kvick, A. *Acta Crystallogr.* **1990**, *B46*, 390.
(8) van der Waals, J. H.; Platteeuw, J. C. *Adv. Chem. Phys.* **1959**, *2*, 1.
(9) Tanaka, H.; Kiyohara, K. *J. Chem. Phys.* **1993**, *98*, 4098.
(10) Tanaka, H.; Kiyohara, K. *J. Chem. Phys.* **1993**, *98*, 8110.
(11) Koga, K.; Tanaka, H.; Nakanishi, K. *J. Chem. Phys.* **1994**, *101*, 3127.
(12) Tanaka, H. *J. Chem. Phys.* **1994**, *101*, 10833.
(13) Bertie, J. E.; Jacobs, S. M. *Can. J. Chem.* **1977**, *55*, 1777.
(14) Bertie, J. E.; Jacobs, S. M. *J. Chem. Phys.* **1982**, *77*, 3230.
(15) Fleyfel, F.; Devlin, J. P. *J. Phys. Chem.* **1988**, *92*, 631.
(16) Tse, J. S.; Powell, B. M.; Sears, V. F.; Handa, Y. P. *Chem. Phys. Lett.* **1993**, *215*, 383.
(17) Tse, J. S.; Klein, M. L.; McDonald, I. R., *J. Chem. Phys.* **1984**, *81*, 6146.
(18) Ratcliffe, C. I.; Ripmeester, J. A. *J. Phys. Chem.* **1986**, *90*, 1259.
(19) Fleyfel, F.; Devlin, J. P. *J. Phys. Chem.* **1991**, *95*, 3811.
(20) Ripmeester, J. A.; Ratcliffe, C. I. *Energy Fuels* **1998**, *12*, 197.
(21) Ikeda, T.; Mae, S.; Uchida, T. *J. Chem. Phys.* **1998**, *108*, 1352.
(22) Ikeda, T.; Fukazawa, H.; Mae, S.; Hondoh, T.; Langway, C. C., Jr. *J. Phys. Chem.* **1997**, *101*, 6180.
(23) Yamamuro, O.; Matsuo, T.; Suga, H.; David, W. I. F.; Ibberson, R. M.; Leadbetter, A. J. Phys. B **1995**, *213&214*, 405.
(24) Kuhs, W. F.; Chazallon, B.; Radaelli, P. G.; Pauer, F. *J. Inclusion Phenom.* **1997**, *29*, 65.
(25) Ikeda, T.; Yamamuro, O.; Matsuo, T.; Mori, K.; Torii, S.; Kamiyama, T.; Izumi, F.; Ikeda, S.; Mae, S. *J. Phys. Chem. Solids* **1999**, *60*, 1527.
(26) Barrer, M.; Edge, A. V. J. *Proc. R. Soc. London* **1967**, *A300*, 1.
(27) Munck, J.; Skjold-Jorgensen, S.; Rasmussen, P. *Chem. Eng. Sci.* **1988**, *43*, 2661.
(28) Ibberson, R. M.; David, W. I. F.; Knight, K. S. *Rutherford Appleton Laboratory Report* **1992** *RAL-92-031*.
(29) Rietveld, H. M. *J. Appl. Crystallogr.* **1969**, *2*, 65.
(30) Ibberson, R. M.; David, W. I. F.; Knight, K. S. *Rutherford Appleton Laboratory Report* **1993** *RAL-92-032*.
(31) Tse, J. S.; McKinnon, W. R.; March, M. *J. Phys. Chem.* **1987**, *91*, 4188.
(32) Yamamuro, O.; Handa, Y. P.; Oguni, M.; Suga, H. *J. Inclusion Phenom.* **1990**, *8*, 45.
(33) Kuhs, W. F.; Lehman, M. S. *J. Physique.* **1987**, *48*, 3.
(34) Peterson, S. W.; Levy, H. A. *Acta Crystallogr.* **1957**, *10*, 70.
(35) Röttger, K.; Endriss, A.; Ihringer, J.; Doyle, S.; Kuhs, W. F. *Acta Crystallogr.* **1994**, *B50*, 644.
(36) Ibach, H.; Lüth, H. In *Festkörperphysik*; Springer: Berlin, 1981.